Probing combinations of acoustic phonons in MoS_2 by intervalley double-resonance Raman scattering

Rafael N. Gontijo, Andreij Gadelha, Orlando J. Silveira, Ricardo W. Nunes, Marcos A. Pimenta, Ariete Righi, and Cristiano Fantini

Departamento de Física, Universidade Federal de Minas Gerais, Belo Horizonte, MG, 31270-901 Brazil

(Received 5 October 2020; revised 12 December 2020; accepted 15 December 2020; published 13 January 2021)

In this work, we present measurements of the temperature dependence of the resonance Raman spectra of MoS_2 in two-dimensional and bulk forms, performed to identify the processes related to different combinations of two acoustic phonons involved in the intervalley scattering. The resonance Raman spectra of samples of different thicknesses (single layer, bilayer, trilayer, and bulk) were measured near the resonance with the *A* excitonic transition and at different temperatures. Measurements of the Raman spectra of bulk MoS_2 were performed using several laser energies across the resonances with the *A* and *B* excitonic transitions. Based on the electronic and vibrational structures of the samples with different thicknesses and the evolution of the bands as a function of the laser excitation energy and temperature, we propose correct assignments to the Raman bands appearing at approximately 380, 395, and 405 cm^{-1}. According to our measurements and data analysis, the peaks at 380, 395, and 405 cm^{-1} correspond to the combinations of 2TA around the **K** point, LA and TA phonons around the **M** point, and LA and out-of-plane acoustic (ZA) phonons around the **M** point, respectively. This work sheds light on the double-resonance processes of MoS_2 and how it is related to the electronic structure of this material. The results presented here establish the assignment and the scattering mechanism for some two-phonon and double-resonance Raman bands whose origins were still a matter of debate in the literature. It can also be an important basis to explain the double-resonance processes in other transition-metal dichalcogenides since we present the fundamental electron scattering mechanism near the resonance with the *A* and *B* excitonic transitions, and how it is affected by thermal effects.

DOI: 10.1103/PhysRevB.103.045411

I. INTRODUCTION

Molybdenum disulfide (MoS_2) is one of the prototypes of two-dimensional (2D) materials that were introduced after the rise of graphene and hexagonal boron nitride [1]. Nowadays, there is a multitude of different 2D materials with different types of properties, and Raman spectroscopy has played a major role to characterize and understand some of their fundamental physical properties [2–7]. Among the different classes of 2D materials, semiconducting transition-metal dichalcogenides (TMDs) have been largely studied by Raman spectroscopy. The Raman spectra of TMDs present a rich structure of features, especially when the laser excitation energy is close to the resonance with an excitonic transition. However, the origin of some features is not entirely understood and different assignments of these features are proposed in the literature. Studies on TMDs to conciliate the various assignments and models for Raman features in literature are still missing.

MoS_2 has been studied using Raman spectroscopy by a myriad of works and its spectrum shows the presence of several Raman features when the laser excitation energy is close to its excitonic transition energies [8–15]. Many works have attempted to explain the origin of the different features observed in the Raman spectra of these materials [8,9,11–13,16]. However, there are still different assignments of the Raman features in the literature. The assignments vary according to the laser lines that are used [8,9,13,17–19], to the number of layers presented in the sample [8,10,11,20], and to the presence of defects and microcrystalline samples [21–23].

Recently some works have been able to distinguish the contributions of the double-resonance bands in MoS_2 due to the combinations of acoustic and optical phonons in the vicinity of the **K** and **M** points of the Brillouin zone [12,13,15]. Different procedures were employed to distinguish the diverse combinations of phonons, where not only the laser energy was changed to observe the behavior of the double-resonance bands, but also measurements at low temperature allowed the observation of other processes.

Livneh and Sterer [9] observed that the frequency of the double-resonance feature commonly known in the literature as the *b* mode, which is a combination of LA and TA phonons [13,15] in the proximities of the **K** point of MoS_2, changes when the temperature is varied at a rate almost three times larger than those of the first-order Raman bands. In this work, it was also observed that the intensity of the first-order A_{1g} mode is strongly affected by thermal effects as well, due to the thermal impact in the electronic structure of the material. Therefore, the variation in the electronic transition energy was responsible for the dispersive behavior of the band, which we also observe for other laser energies and temperatures in our recent work [24]. Livneh and Sterer [9] also reported

 ©2021 American Physical Society

in their work the temperature slopes in the other features at approximately 380, 395, and 403 cm^{-1}, named here as β, γ, and δ peaks, respectively. The β peak appears as a shoulder near the E_{2g} band, while the γ peak exhibits two separate contributions at approximately 393 and 395 cm^{-1}. The β peak was attributed to the phonons in the bottom of the E_{2g} branch, but the γ peak was still unassigned. The δ peak appears as a shoulder of the A_{1g} peak and was assigned to the Raman and IR inactive mode of B_{1u} irreducible representation. By changing the temperature, their frequencies exhibit rates of change similar to those of the first-order A_{1g} and E_{2g} modes. In a latter work [13], Livneh and Spanier also included possible combinations of the acoustic and quasiacoustic bands in the assignment of the β and γ bands, respectively. They proposed that the β band could be associated with either the combination of two TA or TA′ phonons at the **K** point, while the two components of the γ band could be associated with the combinations of LA and TA or LA′ and TA′ phonons at the **M** point.

Gołasa *et al.* [12] measured the Raman spectrum of MoS_2 at 4 K using a 1.96-eV laser and compared it with the spectrum measured at room temperature. They reported the presence of a strong peak in the room-temperature spectrum at approximately 178 cm^{-1}, named here as α, that vanished at low temperature. This result indicated that the α feature could be attributed to a Stokes/anti-Stokes process, in which one optical phonon would be created while an acoustical phonon would be annihilated. The feature was assigned to the difference between an A_{1g} phonon and an LA phonon at the **M** point. The intensity dependence of the α band on temperature is of the form $I \propto (n_{A_{1g}(\boldsymbol{M})} + 1)n_{LA(\boldsymbol{M})}$, where $n_i = [\exp(\hbar\omega_i/KT) - 1]^{-1}$ is the Bose-Einstein occupation factor of a phonon with frequency ω_i [12]. Based on the temperature dependence of I, as T approaches 0, I goes to 0 as well, in perfect agreement with the experimental results. The α peak was also investigated by Chakraborty *et al.* [11], in one, two, four, and seven layers and bulk MoS_2. They observed that the intensity of the α peak is weak for a monolayer sample, but becomes strong for a bilayer, and still stronger for multilayer samples and bulk. However, the difference in the intensity observed between the samples of different thicknesses was not explained.

Recently, Carvalho *et al.* have explored the resonance behavior of single, few-layer, and bulk MoS_2, and measured the intensity and frequency of the double-resonance 2LA and b bands as a function of the excitation laser energy [15]. They observed that the intensity of the double-resonance 2LA band close to the **M** point is stronger for few layers and bulk when compared to the single layer where the b and the 2LA bands close to the **K** point are the dominant double-resonance features. The enhancement of the 2LA band close to the **M** point is a consequence of the appearance of the indirect band gap in n layers and bulk crystals, which can act as an additional scattering channel for the excited electron connecting the **K** and **Q** valleys (**KQ** intervalley scattering). Therefore, we expect that the intensity of the combination processes of acoustic and optical phonons near the **M** points becomes enhanced for n layers and bulk. For a single layer, on the other hand, the scattering of electrons occurs mainly from the **K** valley to the **K′** valley (**KK′** intervalley scattering) and the features can be attributed to combinations of phonons near the **K** point.

The objective of this work is to conciliate the proposed assignments and models in the literature for the combination bands of the resonance Raman spectrum of single-layer (1L), bilayer (2L), trilayer (3L), and bulk MoS_2. The measurements were performed near the resonance with the A exciton (X_A) at room temperature and 80 K with a 1.92-eV laser. The observed difference in the Raman spectra of the samples was explained in terms of the influence of the **KK′** and **KQ** scattering channels in the double-resonance process. We also measured the Raman spectrum of bulk MoS_2 with several laser excitation energies close to X_A and X_B and changing the sample temperature to understand the α, β, γ, and δ Raman features, and how they are affected by these two parameters. We seek to enlighten the contributions of two-phonon processes in the Raman spectra of MoS_2 and other TMDs as well, where similar physical processes are also present. We observe a dispersive behavior of the β, γ, and δ peaks, which allows us to make a correct assignment of the γ and δ peaks associated with the **KQ** scattering. We also explain the low rate of change of the γ and δ peaks as a function of temperature based on the different thermal effects experienced by the **K** and **Q** valleys. Finally, we see how the intensity of the α peak is affected by both the laser excitation energy and temperature effects as well, where the resonance with the excitonic levels becomes as important as the temperature effects, as we show further.

II. EXPERIMENT METHODS

Monolayer (1L), bilayer (2L), trilayer (3L), and bulk samples of MoS_2 were exfoliated from commercial MoS_2 crystals (SPI Supplies) and placed in a Si substrate with a 300-nm oxide layer. The Raman spectroscopy measurements were done in a Horiba T64000 spectrometer in a single-grating configuration for the measurement of the 1.92 eV laser and a triple-grating configuration for the other laser energies used. In both cases, 1800 gr/mm gratings were used. Two lasers are used for the measurements, a Coherent Innova C70 Ar-Kr providing the 1.92 and 2.18 eV laser lines, and a Coherent 899 ring dye laser that could be tuned between 1.94 and 2.21 eV. The sample temperature was controlled by a Linkam THMS600 cryostat in the range from 80 to 300 K. The intensities of the collected spectra were normalized by the intensity of the E_{2g} peak since this mode is nonresonant for laser energies near the energies of X_A and X_B [25,26]. Even in the case of single and few layer, we use the notation of the irreducible representations of the bulk crystals for simplicity. Following our previous work [24], the first-order Raman bands were fitted with Lorentzian peaks, while the double-resonance peaks were fitted with Gaussian peaks.

III. EXPERIMENT RESULTS

A. Raman measurements of single-layer, bilayer, trilayer, and bulk MoS_2 excited near X_A

Figures 1(a) and 1(b) present the Raman spectra of 1L, 2L, 3L, and bulk MoS_2 collected with 1.92 eV laser excitation energy at 300 and 80 K, respectively. At 300 K, the Raman spectra of all samples are dominated by the A_{1g} mode as well

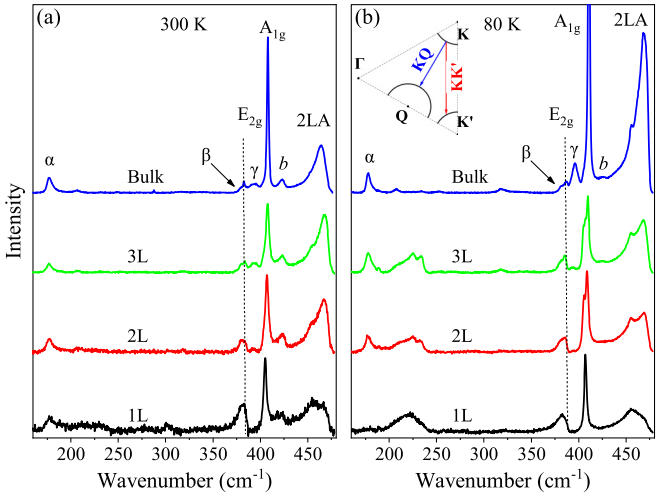

FIG. 1. Raman spectra of 1L, 2L, 3L, and bulk MoS_2 collected with a 1.92-eV laser at the temperatures of (a) 300 and (b) 80 K. The peaks identified by α, β, and γ are discussed in the text. We highlighted the presence of the first-order E_{2g} and A_{1g} modes and the α, β, γ, b, and 2LA bands. The diagram in (b) illustrates (exaggerated) the intervalley scattering of the electron from the vicinity of the **K** point to the vicinity of the **K**′ point (**KK**′) and from the vicinity of the **K** point to the vicinity of the **Q** point.

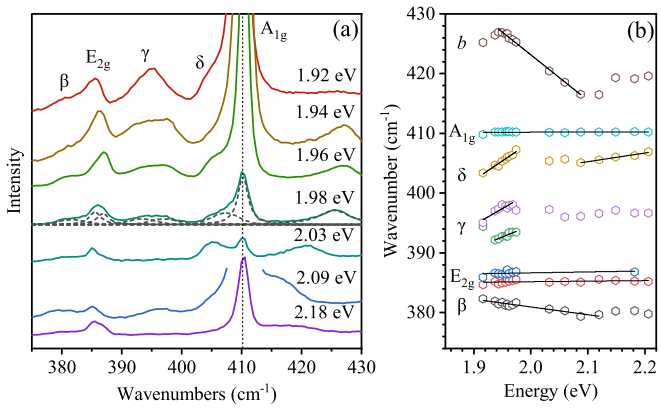

FIG. 2. (a) Raman spectra of bulk MoS_2 collected with laser excitation energies in the range of 1.92 to 2.18 eV at 80 K. The intensity is normalized by the intensity of the E_{2g} mode. The spectrum corresponding to the 1.98-eV laser energy shows the fitting with a sum of Lorentzian and Gaussian peaks, where the γ band was fitted with two Gaussian components. (b) Frequency of the Raman spectral features between 375 and 430 cm^{-1} as a function of the laser excitation energy.

as the double-resonance b and 2LA bands. At 80 K, the Raman spectra are still dominated by the A_{1g} mode, but the spectra of 2L and 3L show a splitting of the A_{1g} band for 2L and 3L due to the additional vibrations that are expected with the increasing number of layers [20,27]. The intensity of the 2LA band for 2L and 3L becomes weaker when compared with the spectra taken at 300 K. For the bulk spectrum, there is a large enhancement of the A_{1g} and 2LA bands at 80 K, where they become ∼50 and ∼14 times more intense than the E_{2g} band, respectively. We also observe in Fig. 1(b) the α, β, and γ features at 178, 380, and 395 cm^{-1}, respectively.

The α band is present in the Raman spectrum of all samples at room temperature, even though it is slightly weaker for 1L than for the other samples. At 80 K, it vanishes for 1L, per the results of Refs. [12,22], but it remains intense for 2L, 3L, and bulk. The β band is pronounced in the Raman spectra of 1L both at room temperature and 80 K. As the number of layers increases to 2L and 3L, the intensity of β decreases, and it becomes just a shoulder of the E_{2g} peak in the bulk spectrum. The γ band is not observed in the spectrum of 1L either at room temperature or at 80 K. Both the spectra of 2L and 3L present a weak γ band at 80 K, which becomes stronger at 300 K. In the bulk spectrum, however, the γ band is strong at room temperature, where its intensity is comparable to the intensity of the E_{2g} band and becomes even stronger at 80 K, where its intensity is almost three times the intensity of the E_{2g} band.

As we will discuss further, the two-phonon processes containing phonons near the **K** point are related to the **KK′** electron scattering, which is strong for 1L and 2L. The two-phonon processes involving phonons in the vicinity of **M** are associated with the **KQ** electron scattering, and these are more pronounced for 2L and even thicker samples, as we could see from Fig. 1. To further understand the **KQ** electron scattering, we needed to make measurements with different laser excitation energies in the energy interval covering the X_A range. In the next section, we present the Raman spectra of bulk MoS_2 obtained with different laser excitation energies and also at different temperatures.

B. Raman measurements of bulk MoS_2 as a function of the laser energy and temperature

Figure 2(a) shows the Raman spectra of bulk MoS_2 measured with laser energies in the range of 1.92 to 2.18 eV at 80 K. The intensity of the A_{1g} band is highly intensified when the laser energy is close to X_A and X_B. The same behavior occurs with the intensity of the b band, where a maximum is reached for laser energies close to X_A and X_B. The plot of the intensity of the A_{1g} band normalized by the intensity of the E_{2g} band as a function of the laser energy can be used to extract the value of X_A and X_B [9,24,25]. This result is used to extract the change of the X_B value as a function of temperature (see Supplemental Material, Fig. S1 [28]).

Figure 2(b) shows the frequency of the bands in the spectral range between 360 and 430 cm^{-1} as a function of the laser energy used. The b band presents a linear slope of −76 cm^{-1}/eV, which is in good agreement with the observed values in the literature for measurements for bulk crystals [17], and 1L of MoS_2 [15,16,24]. The A_{1g} band comes from a zone center out-of-plane phonon and presents no dispersion with the laser excitation energy. The δ band, which appears around 405 cm^{-1}, has slopes of 64 and 14 cm^{-1}/eV in the energy intervals 1.92 to 1.98 eV and 2.09 to 2.21 eV, respectively. We associate it with the combination of LA and TA phonons in the vicinity of the **M** point, as will be discussed further in this text. The γ band presents two components that are nearly degenerate at 1.92 eV and split for higher energies, where a separation of approximately 5 cm^{-1} becomes apparent for the 1.94 eV laser. The higher-energy

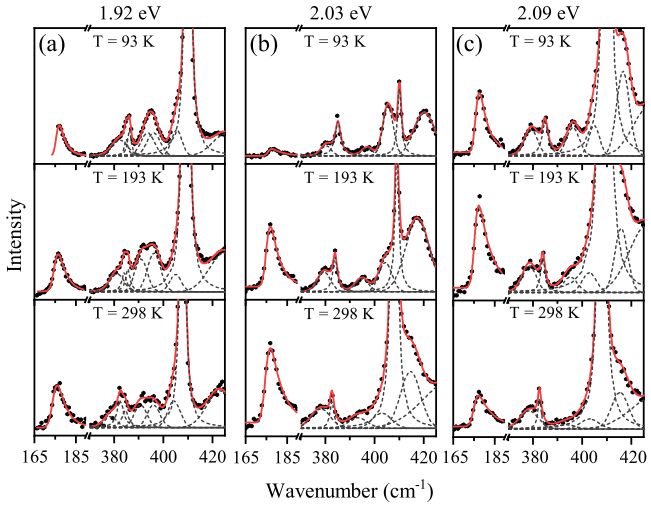

FIG. 3. Raman spectra of bulk MoS_2 in the spectral range of 165 to 430 cm^{-1} at three different temperatures collected with the laser energies of (a) 1.92, (b) 2.03, and (c) 2.09 eV.

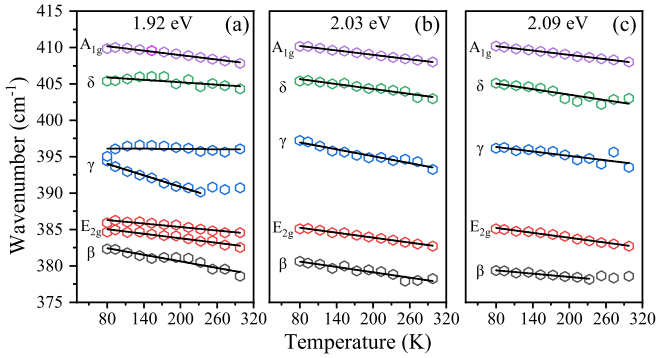

FIG. 4. Frequency of the analyzed bands as a function of temperature of bulk MoS_2 for the (a) 1.92-, (b) 2.03-, and (c) 2.09-eV laser excitation energies. The slopes of the fitting lines are presented in Table I.

component γ' presents a rate of change of 55 cm^{-1}/eV, while the lower-energy component γ'' presents a rate of change of 40 cm^{-1}/eV. Both components of the γ band will be associated with the combination of LA and the out-of plane acoustic (ZA) phonons in the vicinity of the **M** point, as we discuss in details in the next section. The E_{2g} band comes from the degenerate in-plane LO and TO phonons at the **Γ** point. Recent theoretical work [29] has shown that in 2D MoS_2, and any 2D polar material, the LO and TO modes are degenerated at the **Γ** point, and are split for any finite phonon wave vector **q**. In the neighborhood of the **Γ** point, the split depends on the magnitude of **q.** In MoS_2, the theoretical results [29] predict a split on the order 1 cm^{-1}, in very good agreement with the E_{2g} split we obtain in Fig. 2(b). The last set of data in Fig. 2(b) corresponds to the β peak, which presents a slope of -13 cm^{-1}/eV. The β band will be associated with the combination of two TA phonons in the vicinity of the **K** point, as will be explained in the next section. The α band is not included in Fig. 2(b) because it does not present a significative change in frequency, similar to the first-order A_{1g} and E_{2g} modes.

The next step to understand the behavior of the observed peaks is to change the temperature to observe the shifts of the bands as a function of both temperature and laser excitation energy. Figures 3(a)–3(c) show the Raman spectra of bulk MoS_2 in the spectral range of 165 to 430 cm^{-1} collected with the laser energies of 1.92, 2.03, and 2.09 eV, respectively, at the temperatures of 93, 193, and 298 K. Figures 4(a)–4(c) show the frequency of the Raman features of bulk MoS_2 in the spectral range of 165 to 410 cm^{-1} collected with the laser energies of 1.92, 2.03, and 2.09 eV, respectively, at temperatures ranging from 80 to 300 K. Figure 3 shows that the frequency of the α band at 178 cm^{-1} is almost constant throughout all the laser energies and temperatures, but its intensity presents significant changes across the same energy and temperature ranges. As a function of the laser energy, the β band presents a slow decrease in its frequency, and its intensity is almost always small. The γ band presents a split as a function of the laser energy (see Fig. 2), but it also presents a split as a function of the temperature for the 1.92 eV laser energy (see Fig. 4(a)), which is closest to the X_A transition. The δ band presents an increase of its frequency as a function of the laser energy, as it was presented in Fig. 2, but it behaves almost like a first-order mode as a function of temperature (see Figs. 4(a)–4(c)).

A detailed discussion of the experimental data to get the correct assignment of α, β, γ, and δ bands is presented in the next section.

IV. DISCUSSION

The intensity of a Raman process involving the combination of two phonons is given by the equation [30,31]

$$I = C\left|\sum_{a,\,b,c}\frac{\langle f|H_{eR}|c\rangle\langle c|H_{el}|b\rangle\langle b|H_{el}|a\rangle\langle a|H_{eR}|i\rangle}{(\hbar\omega - E_a + i\Gamma)(\hbar\omega - E_b + i\Gamma)(\hbar\omega - E_c + i\Gamma)}\right|^2 \times \begin{cases}(n_1+1)(n_2+1)\\ (n_1+1)n_2\end{cases}, \quad (1)$$

where i represents the initial state of the electron is in the valence band, a, b, and c are intermediate excited states, and f is the final state after the electron-hole recombination. The H_{eR} and H_{el} terms correspond to the electron-radiation and electron-phonon interactions Hamiltonians, respectively. The E_j terms in the denominator ($j = a, b$, or c) correspond to the energy of state j, and Γ is the broadening term that we consider the same for all intermediate states. Given that the electron-phonon interaction H_{el} is weak, the overall intensity of a two-phonon process is weak compared to a first-order Raman process, except when the laser energy matches one or more E_i terms in the denominator of Eq. (1). The phonon occupation factor products, $(n_1+1)(n_2+1)$ and $(n_1+1)n_2$, where $n_i = 1/[\exp(\hbar\omega_i/K_BT) - 1]$, are included for the sum of two phonons and the Stokes/anti-Stokes process, respectively [31]. For simplicity, we have not included the joint density of states in Eq. (1) since the intensity profiles for 2D semiconducting materials with parabolic dispersion can be well described without this contribution.

When two terms in the denominator reach their minimum values, a double-resonance process can be observed. The two terms that become minima depend on the laser excitation energy and whether it is sufficient to excite the electron to the conduction band, create two phonons, and still have more energy than the optical band gap of the material. The sum over all the intermediate states a, b, and c must be considered since the electron can suffer intervalley scattering by phonons within the interior of the Brillouin zone. Therefore, all processes where the electron in the conduction band (or hole in the valence band) is scattered to another real electronic state need to be considered a double-resonance Raman process. The overall intensity of each process depends on factors other than the electronic transition energy, like the electron-phonon interaction term H_{el}. Additionally, the frequency of the phonons that satisfies the double-resonance condition changes according to the wave vector that is accessed by the excited electron in the conduction band. Therefore, it is expected that a double-resonance band may shift according to the laser energy used. Based on Eq. (1), we now move to a deeper discussion of the processes proposed for the α, β, γ, and δ bands.

The α band was previously assigned to the difference between the A_{1g} and LA branches at the **M** point [12,13]. Based on the double-resonance process we propose that it is a process occurring in the vicinity of the **M** point. We base our proposition on the fact that the difference between the A_{1g} and LA branches in the vicinity of the **M** point is flat, confirmed by our theoretical calculations of the phonon structure of bulk MoS_2 (check Supplemental Material, Fig. S2(b) [28]). Therefore, the double-resonance process could present a single frequency, independent of the laser excitation energy.

Due to the nature of thermal effects on the frequency of the α band, we could expect the same result since it corresponds to the difference between two different phonon branches. The created phonon contributes to a negative rate of change as a function of temperature, while the destroyed phonon contributes to a positive rate of change as a function of temperature, yielding a null net rate of change as a function of temperature.

The vital remark we make is about the intensity of the α band, which is incredibly high, even in the low-temperature regime, for the laser energies corresponding to 1.92 and 2.09 eV (Figs. 1 and 3). Based entirely on the occupation factor contained in Eq. (1), the intensity of the Stokes/anti-Stokes process of the α band at 80 K should be only 3% of the observed intensity at 300 K. However, there are still other factors that we must account to properly explain the observed intensity. As such, we use Eq. (1) to calculate the intensity of the α band as a function of both the laser excitation energy, and also as a function of temperature based on the temperature dependence of the excitonic transition energies (more details in the Supplemental Material, section S3). The calculated intensity as a function of the temperature and the laser excitation energy are displayed in Fig. 5(a) as a colored map. We further present the results (multiplied by a constant factor to fit the data) as a function of the laser energy along with the intensities measured at 80 K in Fig. 5(b), where we can observe a good agreement between the experimental data and the calculated results. The same data were used to compare the experimental data at constant laser excitation energies

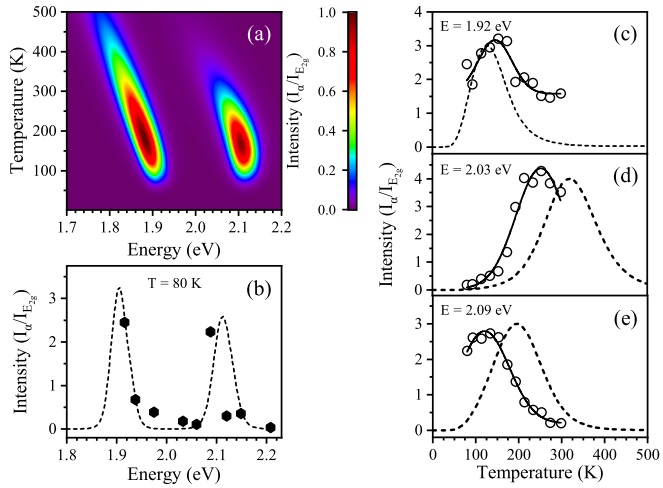

FIG. 5. (a) Colored map showing the calculated intensity of the α band (color scale) as a function of the laser excitation energy (x axis) and the temperature of measurement (y axis). (b) The intensity of the α band as a function of the laser excitation energy. (c), (d), and (e) show the intensity of the α band as a function of temperature for the laser excitation energies of 1.92, 2.03, and 2.09 eV, respectively. The intensities of the experimental data are all normalized by the intensity of the E_{2g} band. The solid lines are a fit with a Gaussian function, while the dashed lines represent the calculated results from (a), at the respective laser excitation energies and temperatures, multiplied by a constant factor to match the intensity observed.

of 1.92, 2.03, and 2.09 eV, as a function of temperature, in Figs. 5(c)–5(e), respectively.

Figure 5(d) shows the intensity of the α band when excited with a 2.03 eV laser as a function of the temperature. The observed behavior is as it is predicted by the product $(n_{A_{1g}(\boldsymbol{M})}+1)n_{LA(\boldsymbol{M})}$, where the intensity at 80 K is approximately 5% of the intensity at 300 K. However, the intensity of the α band measured with the laser excitation energies of 1.92 and 2.09 eV [Figs. 5(c) and 5(e), respectively] is completely different, and the intensities are maximum near the lowest temperature of 80 K. We resort to the simulation proposed in Fig. 5(a) that presents a good qualitative agreement with the experimental data, especially near the resonance with the A exciton, as we can see from Figs. 5(b) and 5(c). The resonance with the B exciton, however, is slightly shifted by approximately 30 meV, which can be observed by comparing the difference in intensity between maximum experimental intensity at 2.09 eV and the maximum simulated intensity at 2.12 eV from Fig. 5(b). This shift is also responsible for the shifted value of the maximum experimental and calculated intensities in Figs. 5(d) and 5(e), where an 80 K shift between the experimental and simulated maxima can be observed. The 80 K shift can be translated to roughly a 30 meV shift in energy according to the rate of change of the A exciton as a function of temperature (approximately -400 μeV/K [32]). Since the shift is apparently constant between our results, we did not include a correction to the simulation because it is not necessary given the simplicity of our model. The conclusion from the comparison between experiment and calculation is that the intensity is affected by temperature, which also affects the excitonic transition energies of X_A and X_B. Therefore, the

simple assumption of the occupation factor is not enough to explain the intensity of the α band, and we also need to resort to the resonance with the excitonic transitions as well.

A critical aspect of the α band is the difference in intensity between 1L and the other samples, which we showed in Fig. 1. To understand the reason why this band is so strong for 2L, 3L, and bulk, we resort to the **KQ** scattering channel, which also explains the high intensity of the 2LA band in 2L, 3L, and bulk [15]. The **Q** valley in the conduction band is actually above the alignment with the **K** (or **K′**) valley in the 1L sample. Therefore, unless the excitation energy is high enough, it is not possible to observe the associated process as a strong band, since it is not doubly resonant. As the number of layers increases, however, the **Q** valley in the conduction band shifts to lower energy. Since the energy shift brings the two valleys closer together, it is possible to attain a double-resonance process in this case, since the phonons involved will be able to connect the electronic states in these two valleys.

Another important point to consider is how the energy of the **Q** valley is affected by temperature, given its importance for the double-resonance processes in MoS_2. Recently, the photoluminescence (PL) emission of a bilayer MoS_2 was measured as a function of temperature [31], and two main observations must be highlighted. The transition energy of the excitons X_A and X_B and the A trion decreased as a function of temperature, which is a known result for single-layer and bulk MoS_2 [24,33–36], but the indirect band gap, connecting the **Γ** point in the valence band to the **Q** point in the conduction band, is increased as a function of temperature. This observation means that the valley around the **Q** point is being displaced to higher energies as the temperature increases. This result was also observed in another TMD in the semiconducting 2H family, namely WS_2 [37]. Recently, the PL spectra of bulk MoS_2 were measured as a function of temperature in the range between 80 and 250 K [38], and those measurements suggest a similar behavior as well. Therefore, thermal effects act differently in the valleys around the **K** and **Q** points, where the **K** (**Q**) valley energy decreases (increases) for increasing temperature values.

In practice, if we measure the Raman spectrum near the resonance with X_A at a low temperature, 80 K, and high temperature, 300 K, the resonance with the **KQ** scattering channel will be affected according to the number of layers in the sample. This means that while the intensity of the 2LA band is close between 2L, 3L, and bulk at 300 K, at 80 K, it will be out of resonance for 2L and 3L and still in resonance for bulk (see Fig. 1). The α band, coming from a Stokes/anti-Stokes process, will not be affected as much because the phonon being destroyed can connect the electron to the former electronic state, which will remain a double-resonance process, except in a 1L sample.

The β band is present in all samples in Fig. 1, and it is a strong band for 1L and 2L but it becomes weaker in 3L while it is weakest for bulk, independent of temperature as well. In Fig. 2(b), we showed that the β band changes as a function of the laser energy at a rate of $-13\,\mathrm{cm}^{-1}/\mathrm{eV}$. Compared with the rate of change of the b band, this is a small rate of change. The two possible assignments of the β band proposed by Ref. [13] are the combination of two TA or TA′ phonons at the **K** point. The dispersive behavior of the β band, however, suggests that it is a process occurring in the vicinity of the **K** point. Additionally, the fact that we can see this process regardless of the thickness of the sample (1L, 2L, 3L, and bulk) naturally allows the correct assignment of the β band to the combination of two TA phonons around the **K** point.

The γ band is one of the most interesting features in the Raman spectrum of MoS_2. At 80 K, it is inexistent for 1L and it gradually becomes more intense from 2L to 3L to bulk, where it is maximum. At room temperature, its intensity is close for 3L and bulk, while still weak for 2L and inexistent for 1L. Also, at 80 K, it is present as a single peak in 2L, 3L, and bulk, but it splits for these three samples at room temperature. The proposed assignment of the two components of the γ band according to Ref. [13] is the combination of an LA phonon and a TA phonon near the **M** point (γ') and the combination of an LA′ and a TA′ phonon near the **M** point (γ''). Although the assignment is in qualitative agreement with the observed frequencies of the γ band at laser energies above 1.92 eV in Fig. 2(b), it cannot explain the crossing of the two components of the peak at 1.92 eV, because the quasiacoustic bands are well separated from the acoustic bands by approximately $3\,\mathrm{cm}^{-1}$ [check Supplemental Material, Fig. S2(a)]. However, if we can allow the possibility of more than one scattering channel to the vicinities of the **Q** valley, we may be able to explain the existence of the two components. We illustrate this process in the Supplemental Material (Fig. S4). Since the frequency of the two components is increasing as a function of the laser energy [see Fig. 2(b)], but at a lower rate than the δ band, we propose the combination of an LA phonon and a ZA phonon in the vicinity of the **M** point. Since the electron-phonon interaction of the ZA phonons is small (lack of a 2ZA feature near the **K** or **M** points), the overall intensity of this process is significantly diminished. We can compare the intensity difference of this process to the intensity difference of the $2D$ and $2D'$ bands in graphene [39].

The last remaining peak is the δ band at approximately $403\,\mathrm{cm}^{-1}$, which is often assigned to the Raman and IR inactive B_{1u} phonon at the **Γ** point. The measurements of the position of this peak as a function of the laser energy in our work show that it presents a positive rate of change of $64\,\mathrm{cm}^{-1}/\mathrm{eV}$ in the energy interval between 1.92 and 1.98 eV [Fig. 2(b)]. The presented rate of change is high, and also inconsistent with the current assignment proposed for this band.

The δ band is weak present only in the bulk sample (Fig. 1). The band could potentially be assigned to the **KQ** scattering given that the electron-phonon interaction responsible for this band is small. This is supported by the fact that we cannot see this band in the 1L, 2L, or 3L spectra (see Fig. 1), and it is only present in the bulk sample spectrum. According to the frequency and the high positive rate of change of the δ band, we can assign it to the combination of LA and TA phonons in the vicinity of the **M** point. The low intensity of this band can also be explained by the weak electron-phonon interaction of the TA branch near the **M** point since the 2TA(∼**M**) band is weak compared to the electron-phonon interaction of the LA branch. Also, in few-layer samples (2L, 3L, 4L, and thicker samples), there is the presence of the other A_{1g}-like modes [20,27], which are much more intense than the γ band, and can hide the existence of other possible features in the same spectral range.

TABLE I. Raman frequencies and their respective slopes as a function of temperature of bulk MoS_2.

$\omega(\mathrm{cm}^{-1})$	Name	$(\frac{\partial\omega}{\partial T})_{E=1.92\,\mathrm{eV}}(\mathrm{cm}^{-1}/\mathrm{K})$	$(\frac{\partial\omega}{\partial T})_{E=2.03\,\mathrm{eV}}(\mathrm{cm}^{-1}/\mathrm{K})$	$(\frac{\partial\omega}{\partial T})_{E=2.09\,\mathrm{eV}}(\mathrm{cm}^{-1}/\mathrm{K})$	Assignment
380	β	−0.015(2)	−0.012(1)	−0.008(1)	2TA(∼**K**)
384	E_{2g}	−0.010(1)	−0.011(1)	−0.011(1)	
395	γ	−0.026(2)	−0.016(1)	−0.010(2)	LA+ZA(∼**M**)
403	δ	−0.006(2)	−0.011(1)	−0.013(2)	LA+TA(∼**M**)
410	A_{1g}	−0.010(1)	−0.010(1)	−0.010(1)	

Our discussion above provides satisfactory explanations to the β, γ, and δ bands when we consider their frequency as a function of the laser energy and keep the temperature fixed. However, we still need to address the rate of change of their position as a function of temperature, which is affected in approximately the same way as the first-order A_{1g} and E_{2g} bands (see Figs. 4(a)–4(c) and Table I), inconsistent with a two-phonon assignment.

We use the following equation to describe the change observed in the frequency of a double-resonance band ω_i as a function of temperature:

$$\left(\frac{\partial\omega_i}{\partial T}\right)_{\hbar\omega} = -\left(\frac{\partial\omega_i}{\partial\hbar\omega}\right)_T\left(\frac{\partial E_g}{\partial T}\right)_{\hbar\omega} + \left(\frac{\partial\omega_i}{\partial T}\right)_{\Delta E}, \quad (2)$$

where $\hbar\omega$ is the laser energy, $\Delta E = \hbar\omega - E_g$, and E_g corresponds to the excitonic transition energy X_A. The details for obtaining Eq. (2) are included in the Supplemental Material, section S5. Equation (2) combines two effects that are observed when the temperature is changed, the effect of resonance with the electronic level on the two-phonon process, $(\frac{\partial\omega_i}{\partial\Delta E})_T(\frac{\partial E_g}{\partial T})_{\hbar\omega}$, and the change in the vibrational energies due to anharmonic effects, $(\frac{\partial\omega_i}{\partial T})_{\Delta E}$.

We can look into Eq. (2) to discuss the position of the β, γ, and δ bands as a function of temperature. For the **KK′** scattering, we need only consider the rate of change of the excitonic transition X_A, to see how the **K** valley is affected by temperature. According to the results from bilayer MoS_2 in Ref. [32], X_A presents a rate of change of approximately −400 μeV/K between 100 and 300 K, and we use this result for our bulk sample. The rate of change of β as a function of the laser energy is $-13\,\mathrm{cm}^{-1}/\mathrm{eV}$, and combining these two results, we obtain $(\frac{\partial\omega_i}{\partial\Delta E})_T(\frac{\partial E_g}{\partial T})_{\hbar\omega} = 0.005\,\mathrm{cm}^{-1}/\mathrm{K}$. From the results obtained near the resonance with X_A (Table I), we see that $(\frac{\partial\omega_i}{\partial T})_{1.92\,\mathrm{eV}} = -0.015\,\mathrm{cm}^{-1}/\mathrm{K}$. Therefore, we obtain $(\frac{\partial\omega_i}{\partial T})_{\Delta E} = -0.010\,\mathrm{cm}^{-1}/\mathrm{K}$. Since the β band is composed of two TA phonons near the **K** point, we conclude that $(\frac{\partial\omega_{\mathrm{TA}(\sim\boldsymbol{K})}}{\partial T})_{\Delta E} = 0.005\,\mathrm{cm}^{-1}/\mathrm{K}$. This result is half the value observed for the first-order A_{1g} mode (see Table I), and also smaller than the value we previously observed for a 1L sample [24]. The stiffening may be caused by the presence of the other layers.

The **KQ** scattering takes the electron from the **K** valley to the **Q** valley, and in this case, we need to consider the dependence of both valleys′ energies with temperature. The **K** valley changes at a rate of −400 μeV/K, but the **Q** valley changes at a rate of 420 μeV/K [32]. Combining the two rates in the term $(\frac{\partial E_g}{\partial T})_{\hbar\omega}$ yields a net value of approximately 20 μeV/K, which is negligible within the precision of the experiment. Therefore, only the second term on the right-hand side of Eq. (2) is important, and it directly relates the changes in the measured frequency of the Raman bands with the change due to thermal anharmonic effects.

Assuming that the change in frequency is equal between the acoustic phonons around the **M** point, and using the result of $(\frac{\partial\omega_\gamma}{\partial T})_{2.03\,\mathrm{eV}} \approx (\frac{\partial\omega_\delta}{\partial T})_{2.03\,\mathrm{eV}} \approx -0.012\,\mathrm{cm}^{-1}/\mathrm{K}$, we obtain that $(\frac{\partial\omega_{\mathrm{LA}(\sim\boldsymbol{M})}}{\partial T})_{\hbar\omega} = (\frac{\partial\omega_{\mathrm{TA}(\sim\boldsymbol{M})}}{\partial T})_{\hbar\omega} = (\frac{\partial\omega_{\mathrm{ZA}(\sim\boldsymbol{M})}}{\partial T})_{\hbar\omega} = -0.006\,\mathrm{cm}^{-1}/\mathrm{K}$, which is 30% smaller than the rate of the first-order optical modes. We use the laser energy of 2.03 eV as a reference here since the γ band presents only a single component after 1.98 eV.

V. CONCLUSION

In conclusion, we presented the Raman spectra of 1L, 2L, 3L, and bulk MoS_2 collected with a 1.92 eV laser line, directly in resonance with the X_A excitonic transition, at two different temperatures, as well as the Raman spectra of bulk MoS_2 collected with different laser excitation energies and different temperatures. Analyzing MoS_2 samples with different thicknesses at varied excitation laser energies, and temperatures, we observed how the Raman spectra of MoS_2 were affected by the different electronic structure configurations and explain the scattering mechanism responsible for the bands named here as α, β, γ and δ. From our experiments, we were able to associate the β, γ, and δ bands with intervalley processes involving acoustic phonons, where the β band can be associated with the 2TA around **K** process, the γ band can be associated with the LA+ZA around **M** process, and the δ band can be associated with the LA+TA around **M** process. The **KQ** scattering becomes stronger for thicker samples, but since the **K** and **Q** valleys are affected differently by thermal effects, some double-resonance processes can present a softening similar to a first-order mode.

The results obtained from our analysis of the different number of layers allowed the correct assignments of the β, γ, and δ Raman bands in bulk (see Table I), which were previously attributed to several possible processes or Raman-inactive phonons and could be reduced to a single possible process in all cases. Additionally, we showed that the Stokes/anti-Stokes process of the α band in TMDs is strongly affected by the resonance with the excitonic transitions and also by the **KQ** scattering process, where the intensity of this mode is weak for a monolayer and strong for any other sample thickness for laser excitation energies close to X_A.

ACKNOWLEDGMENTS

This work was supported by the Instituto Nacional de Ciência e Tecnologia (INCT) em Nanomateriais de Carbono

(Federative Republic of Brazil), Coordenação de Aperfeiçoamento de Pessoal de Nível Superior (CAPES, Federative Republic of Brazil), Conselho Nacional de Desenvolvimento Científico e Tecnológico (CNPq, Federative Republic of Brazil), FINEP (Financiadora de Inovação e Pesquisa), and Fundação de Amparo à Pesquisa do Estado de Minas Gerais (FAPEMIG, Federative Republic of Brazil). R.N.G. acknowledges the post-doc fellowship from CAPES/Brasil. C.F. acknowledges financial support from CNPq (Grants 307742/2017-2 and 432384/2018-9).

[1] K. S. Novoselov, D. Jiang, F. Schedin, T. J. Booth, V. V. Khotkevich, S. V. Morozov, and A. K. Geim, Proc. Natl. Acad. Sci. **102**, 10451 (2005).
[2] H. B. Ribeiro, M. A. Pimenta, and C. J. S. de Matos, J. Raman Spectrosc. **49**, 76 (2018).
[3] G. Froehlicher, E. Lorchat, O. Zill, M. Romeo, and S. Berciaud, J. Raman Spectrosc. **49**, 91 (2018).
[4] J. van Baren, G. Ye, J.-A. Yan, Z. Ye, P. Rezaie, P. Yu, Z. Liu, R. He, and C. H. Lui, 2D Mater. **6**, 025022 (2019).
[5] J.-U. Lee and H. Cheong, J. Raman Spectrosc. **49**, 66 (2018).
[6] S. Zhang, N. Zhang, Y. Zhao, T. Cheng, X. Li, R. Feng, H. Xu, Z. Liu, J. Zhang, and L. Tong, Chem. Soc. Rev. **47**, 3217 (2018).
[7] J. Xie, D. Zhang, X.-Q. Yan, M. Ren, X. Zhao, F. Liu, R. Sun, X. Li, Z. Li, S. Chen, Z.-B. Liu, and J.-G. Tian, 2D Mater. **6**, 035011 (2019).
[8] M. Placidi, M. Dimitrievska, V. Izquierdo-Roca, X. Fontané, A. Castellanos-Gomez, A. Pérez-Tomás, N. Mestres, M. Espindola-Rodriguez, S. López-Marino, M. Neuschitzer, V. Bermudez, A. Yaremko, and A. Pérez-Rodríguez, 2D Mater. **2**, 035006 (2015).
[9] T. Livneh and E. Sterer, Phys. Rev. B **81**, 195209 (2010).
[10] H. Li, Q. Zhang, C. C. R. Yap, B. K. Tay, T. H. T. Edwin, A. Olivier, and D. Baillargeat, Adv. Funct. Mater. **22**, 1385 (2012).
[11] B. Chakraborty, H. S. S. R. Matte, A. K. Sood, and C. N. R. Rao, J. Raman Spectrosc. **44**, 92 (2013).
[12] K. Gołasa, M. Grzeszczyk, P. Leszczyński, C. Faugeras, A. A. L. Nicolet, A. Wysmołek, M. Potemski, and A. Babiński, Appl. Phys. Lett. **104**, 092106 (2014).
[13] T. Livneh and J. E. Spanier, 2D Mater. **2**, 035003 (2015).
[14] B. R. Carvalho, L. M. Malard, J. M. Alves, C. Fantini, and M. A. Pimenta, Phys. Rev. Lett. **114**, 136403 (2015).
[15] B. R. Carvalho, Y. Wang, S. Mignuzzi, D. Roy, M. Terrones, C. Fantini, V. H. Crespi, L. M. Malard, and M. A. Pimenta, Nat. Commun. **8**, 14670 (2017).
[16] J. Kutrowska-Girzycka, J. Jadczak, and L. Bryja, Solid State Commun. **275**, 25 (2018).
[17] T. Sekine, K. Uchinokura, T. Nakashizu, E. Matsuura, and R. Yoshizaki, J. Phys. Soc. Japan **53**, 811 (1984).
[18] T. Sekine, T. Nakashizu, E. Matsuura, and K. Uchinokura, in *Proceedings of the IXth International Conference on Raman Spectroscopy* (Chemical Society of Japan, Tokyo, 1984), pp. 228–229.
[19] A. M. M. Stacy and D. T. T. Hodul, J. Phys. Chem. Solids **46**, 405 (1985).
[20] W. Na, K. Kim, J.-U. Lee, and H. Cheong, 2D Mater. **6**, 015004 (2018).
[21] N. T. McDevitt, J. S. Zabinski, M. S. Donley, and J. E. Bultman, Appl. Spectrosc. **48**, 733 (1994).
[22] G. L. Frey, R. Tenne, M. J. Matthews, M. S. Dresselhaus, and G. Dresselhaus, Phys. Rev. B **60**, 2883 (1999).
[23] S. Mignuzzi, A. J. Pollard, N. Bonini, B. Brennan, I. S. Gilmore, M. A. Pimenta, D. Richards, and D. Roy, Phys. Rev. B **91**, 195411 (2015).
[24] R. N. Gontijo, A. Gadelha, O. J. Silveira, B. R. Carvalho, R. W. Nunes, L. C. Campos, M. A. Pimenta, A. Righi, and C. Fantini, J. Raman Spectrosc. **50**, 1867 (2019).
[25] B. R. Carvalho, L. M. Malard, J. M. Alves, C. Fantini, and M. A. Pimenta, Phys. Rev. Lett. **116**, 089904 (2016).
[26] T. Sekine, T. Nakashizu, M. Izumi, K. Toyoda, K. Uchinokura and E. Matsuura, *Proceedings of the 15th International Conference on the Physics of Semiconductors*, Physical Society of Japan, Vol. 49 (Journal of the physical society of Japan, Kyoto, 1980) Suppl. A, p 551–554.
[27] J. Ribeiro-Soares, R. M. Almeida, E. B. Barros, P. T. Araujo, M. S. Dresselhaus, L. G. Cançado, and A. Jorio, Phys. Rev. B **90**, 115438 (2014).
[28] See Supplemental Material at http://link.aps.org/supplemental/10.1103/PhysRevB.103.045411 for measurements of the *B* exciton energy as a function of temperature; phonons dispersion of bulk MoS_2; simulation of the intensity profile of the α band as a function of the laser energy and temperature; diagram for possible electron scattering processes, and the mathematical development of Eq. (2).
[29] T. Sohier, M. Gibertini, M. Calandra, F. Mauri, and N. Marzari, Nano Lett. **17**, 3758 (2017).
[30] R. N. Gontijo, G. C. Resende, C. Fantini, and B. R. Carvalho, J. Mater. Res. **34**, 1976 (2019).
[31] M. Cardona, R. K. Chang, G. Güntherodt, M. B. Long, and H. Vogt, *Light Scattering in Solids II* (Springer, Berlin, 1982).
[32] L. Du, T. Zhang, M. Liao, G. Liu, S. Wang, R. He, Z. Ye, H. Yu, R. Yang, D. Shi, Y. Yao, and G. Zhang, Phys. Rev. B **97**, 165410 (2018).
[33] C. H. Ho, C. S. Wu, Y. S. Huang, P. C. Liao, and K. K. Tiong, J. Phys.: Condens. Matter **10**, 9317 (1998).
[34] P. Dey, J. Paul, Z. Wang, C. E. Stevens, C. Liu, A. H. Romero, J. Shan, D. J. Hilton, and D. Karaiskaj, Phys. Rev. Lett. **116**, 127402 (2016).
[35] T. Korn, S. Heydrich, M. Hirmer, J. Schmutzler, and C. Schüller, Appl. Phys. Lett. **99**, 102109 (2011).
[36] A. A. Mitioglu, K. Galkowski, A. Surrente, L. Klopotowski, D. Dumcenco, A. Kis, D. K. Maude, and P. Plochocka, Phys. Rev. B **93**, 165412 (2016).
[37] M. R. Molas, K. Nogajewski, A. O. Slobodeniuk, J. Binder, M. Bartos, and M. Potemski, Nanoscale **9**, 13128 (2017).
[38] O. O. Smirnova, I. A. Eliseyev, A. V Rodina, and T. V Shubina, J. Phys. Conf. Ser. **1482**, 012038 (2020).
[39] P. Venezuela, M. Lazzeri, and F. Mauri, Phys. Rev. B **84**, 035433 (2011).